

# Computational Imaging Project Report

Xinyi Huang

## 1 Introduction

The relentless pursuit of medical imaging excellence has led to the exploration of deep learning paradigms that push the boundaries of speed and fidelity. This project report unfurls the narrative of three deep learning models: VARNET, MODL, and SSDU, each a protagonist in its own right within the arena of accelerated magnetic resonance imaging (MRI) reconstruction. Bridging the chasm between high-speed imaging requirements and high-fidelity outcomes, these models stand at the confluence of innovation and clinical application.

The report delineates the theoretical underpinnings that form the bedrock of these models, marrying classic variational models with the adaptability of deep learning to create a symphony of algorithms designed for efficacy. In the heart of this exploration lies a dataset—a tapestry of clinical imaging data that serves as the battleground for these algorithms to prove their mettle. Each model, with its unique architecture, strives to reconstruct clinical accelerated multi-coil MRI data with unprecedented speed, without sacrificing the sanctity of the image quality.

The iterative processes that define these models, the self-learning and self-improving nature of their frameworks, and their integration into clinical workflows represent a leap towards the future of medical imaging. The report presents an empirical evaluation of the models against a rigorous metric of quality and speed, offering a granular view of their performance across varying parameters.

In essence, this project report is a chronicle of the confluence of deep learning with computational imaging, set against the backdrop of the modern medical imaging landscape. It is a testament to the potential of artificial intelligence to enhance patient care by transcending traditional imaging limitations.

## 2 Theory

### 2.1 VARNET

The Variational Network (VN) for MRI Reconstruction [1], as outlined in the document, is an advanced learning-based approach that integrates the principles of variational models with deep learning techniques to improve the reconstruction of accelerated MRI data. The goal is to achieve fast, high-quality reconstruction of clinical accelerated multi-coil MRI data by learning a variational network. This network combines the mathematical framework of variational models with the adaptability and efficiency of deep learning.

**Theory** Variational Model and Deep Learning Integration: The VN approach embeds a generalized compressed sensing (CS) reconstruction, formulated as a variational model, within a deep learning framework. This integration leverages the structured approach of variational models with the learning capabilities of deep networks.

**Gradient Descent Scheme:** The method uses an “unrolled” gradient descent scheme for the iterative solution, where the parameters (including filter kernels, activation functions, and data term weights) of the variational model are learned during an offline training procedure.

**Learning from Data:** Instead of solving a new optimization problem for each exam or reconstruction task, the VN learns from a set of training data, optimizing the parameters for the inverse transform in advance. This pre-learned model is then applied to new, unseen data efficiently.

**Implementation** Parameter Learning: Parameters are learned from training data, which involves comparing the VN’s current reconstruction output to artifact-free reference images and adjusting parameters to minimize reconstruction error.

**Efficiency and Integration into Clinical Workflow:** The learned model can be applied online to previously unseen data, allowing for quick reconstruction times (193 ms mentioned for a specific dataset) and the potential for easy integration into clinical workflows without the need for parameter tuning once the network is trained.

**Superior Performance:** The VN reconstructions outperformed standard reconstruction algorithms in tests, preserving the natural appearance of MR images and accurately depicting pathologies not included in the training set.

## 2.2 MODL

The MODL (Model-Based Deep Learning) framework introduced by Hemant K. Aggarwal, Merry P. Mani, and Mathews Jacob is a pioneering approach in the domain of medical imaging [2], particularly aimed at enhancing image reconstruction from sparse or incomplete datasets. This document outlines the architecture, motivation, and potential applications of MODL, shedding light on its significance in the advancement of medical imaging technology.

**Theory** MODL is presented as a novel framework that marries the strengths of model-based image reconstruction techniques with the power of deep learning, specifically convolutional neural networks (CNNs). At the heart of MODL is the idea of using CNNs to serve as a regularization prior in the image reconstruction process. This integration acknowledges the capability of CNNs to capture complex image features and structures, which are then used to guide the reconstruction of images from undersampled (sparse) data.

The framework employs an iterative process where a CNN-based regularization is alternated with data consistency steps, ensuring the reconstructed image adheres both to the measured data and to the learned image representations. This iterative process is formulated as an optimization problem, with the forward model of the imaging system explicitly accounted for. This explicit consideration allows for a more efficient and effective reconstruction, particularly when dealing with complex imaging systems like MRI.

**Implementation** The MODL framework holds significant potential for a wide range of medical imaging applications, particularly in scenarios where the available data are sparse or incomplete. This includes accelerated MRI, where reducing scan time is of paramount importance, and in dynamic imaging scenarios where capturing fast physiological changes is crucial. By providing a means to reconstruct high-quality images from limited data, MODL can contribute to faster, safer, and more efficient imaging procedures, ultimately enhancing patient care.

## 2.3 SSDU

The SSDU (Self-Supervised Learning via Data Undersampling) model [3], as detailed in the paper "Self-supervised learning of physics-guided reconstruction neural networks without fully sampled reference data" by Burhaneddin Yaman and colleagues, proposes an innovative strategy for training MRI reconstruction neural networks. This model is designed to function in the absence of a fully sampled dataset, addressing a significant challenge in the medical imaging field, particularly for MRI where acquiring fully sampled data can be time-consuming or impractical.

**Theory** The SSDU model leverages self-supervised learning, utilizing a novel training strategy that does not rely on fully sampled ground-truth data. This approach divides available measurements into two disjoint sets. One set is employed in the data consistency (DC) units within the unrolled network architecture, while the other set is used to define the training loss. This division enables the model to learn from partially sampled data effectively.

The architecture of the SSDU framework includes:

Physics-guided deep learning reconstruction, integrating knowledge of MRI's forward encoding process. It solves the inverse problem based on a regularized least-squares objective function.

An iterative process where the CNN-based regularization is alternated with data consistency steps, ensuring that the reconstructed image adheres to the measured data and the learned image representations.

The model uses convolutional neural networks (CNNs) as a regularization prior, leveraging CNNs’ ability to capture complex image features and structures to guide image reconstruction from undersampled data.

**Implementation** The SSDU model was evaluated using the publicly available fastMRI knee database and compared with fully supervised training methods and conventional compressed-sensing and parallel imaging methods. The results demonstrated that SSDU:

Achieves comparable performance with supervised learning models trained on fully sampled data.

Significantly outperforms conventional compressed-sensing and parallel imaging methods, as validated by quantitative metrics and a clinical reader study.

Exhibits flexibility by applying to different acceleration rates and prospectively two-fold accelerated high-resolution brain datasets, showcasing its robustness and effectiveness in real-world scenarios.

### 3 Dataset Description

**Original fastmri data keys** 'ismrmrd\_header', 'kspace', 'reconstruction\_rss'.

**Chose Data** Randomly select 15 t2 weighted H5 files, of which 12 are for training and 3 for testing, maintaining a training to testing ratio of 4:1. Consequently, the dataset comprises 192 training data and 48 testing data.

**Kspace Processing** Extract the 'kspace' from the raw data to obtain the kspace for each slice, and normalize the kspace:

$$k = \frac{k}{\max(|k|)} \tag{1}$$

**trnOrg and tstOrg** Perform an inverse Fourier transform on the kspace to obtain the original image, denoted as 'org'.

**Dataset creators** Please list anyone who helped to create the dataset (who may or may not be an author of the data paper), including their roles (using and affiliations).

**trnMask and tstMask** Select Poisson as the undersampling mask with an acceleration rate of 6.

**trnCsm and tstCsm** Use ESPIRiT6 [4] to calculate coil sensitivity maps.

**Date processing** Create a new H5 file as Modl\_data, which contains the keys: 'trnCsm', 'trnMask', 'trnOrg', 'tstCsm', 'tstMask', and 'tstOrg'.

## 4 Methods

### 4.1 VARNET

The update rule in VARNET [1]:

$$z = x^{(t)} - \lambda A^H (Ax^{(t)} - y) \tag{2}$$

$$x^{(t+1)} = z - \mathcal{N}_\theta^{(t)}(z) \tag{3}$$

where  $t$  is cascade index,  $A$  is forward operator,  $y$  is measured  $k$ -space data and  $\mathcal{N}_\theta^{(t)}$  is U-Net.

The data consistency(DC) module is constructed by equation(2), a sequence of U-Net neural network models is constructed by PyTorch. Consequently Fig.1 presents the configuration of the Variational Network (VN), which is composed of  $T$  iterative steps of gradient descent. For the purpose of reconstruction, inputs such as subsampled  $k$ -space data, coil sensitivity maps, and zero-filled solutions are fed into the VN. Herein, we provide a detailed illustration of a representative gradient step. Considering the complex

nature of the images in question, distinct filters  $k_i^t$  are deduced for both the real and imaginary components. The non-linear activation function  $\phi_i^t$  is responsible for merging the filter responses from these two characteristic planes. Throughout the training process, parameters including filter kernels, activation functions, and the weights of the data term  $\lambda^t$  are subject to optimization.

As Figure.2 shows, the training procedure for the Variational Network involves learning a collection of parameters for the VN during an offline training routine. To achieve this, the current VN reconstruction is benchmarked against an artifact-free reference by employing a metric of similarity. This process yields the reconstruction error, which is then relayed back into the VN for the calculation of a renewed set of parameters.

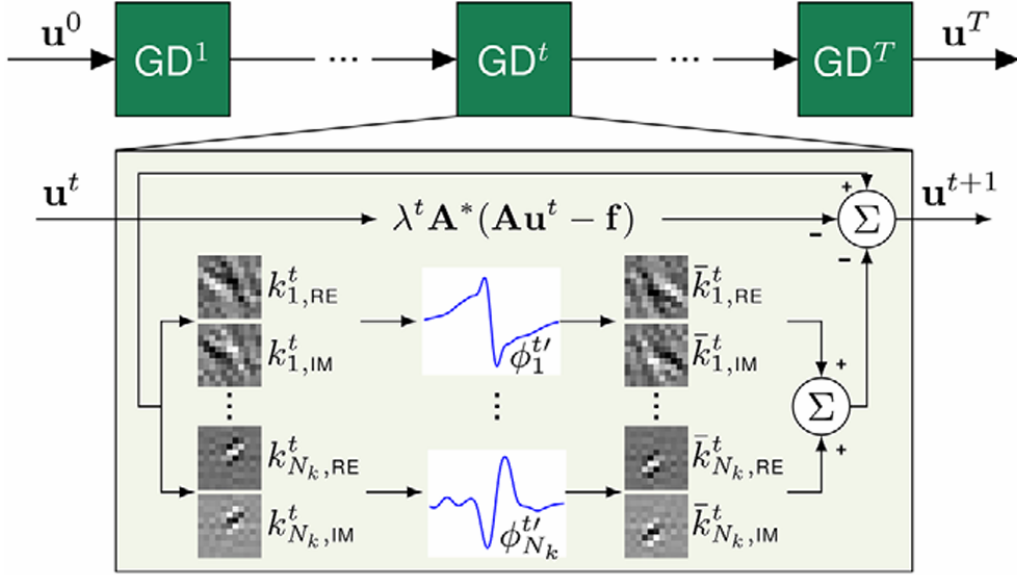


Figure 1: Structure of the variational network (VN).

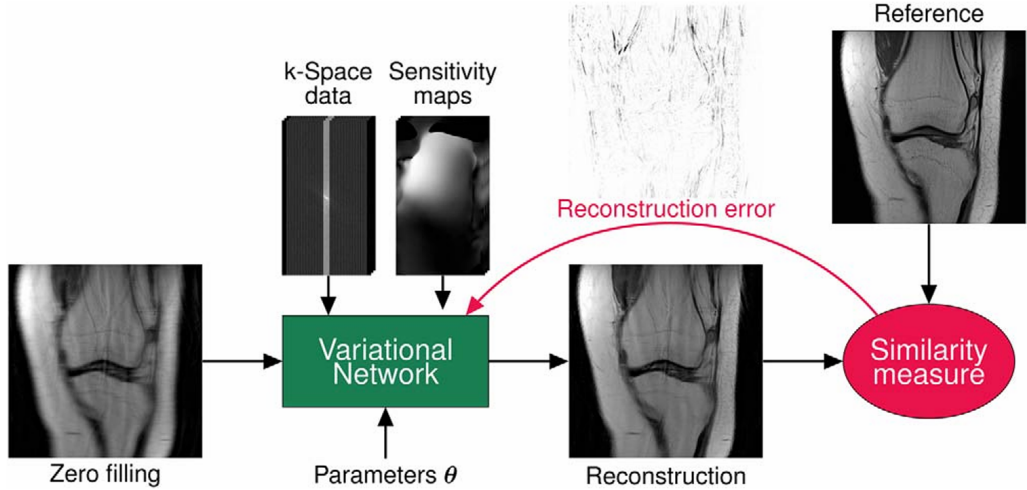


Figure 2: Variational network training procedure.

## 4.2 MODL

The optimization problem in MODL:

$$X_{\text{rec}} = \arg \min \|A(x) - b\|_2^2 + \lambda \|\mathcal{N}_w(x)\|_2^2. \quad (4)$$

where  $n$  is cascade index,  $A$  is forward operator,  $b$  is measured  $k$ -space data and  $\mathcal{N}_w$  is a learned CNN estimator of noise and alias patterns, which depends on the learned parameters  $w$ .

$\mathcal{N}_w$  is expressed as

$$\mathcal{N}_w(x) = (\mathcal{I} - D_w)(x) = x - D_w(x). \quad (5)$$

where  $\mathcal{N}_w(x)$  is the ‘‘denoised’’ version of  $x$ , after the removal of alias artifacts and noise. SO alternating algorithm is approximated as

$$x_{n+1} = \arg \min_x \|A(x) - b\|_2^2 + \lambda \|x - z_n\|_2^2, \quad (6)$$

$$z_n = D_w(x_n) \quad (7)$$

where  $\lambda$  is a trainable regularization parameter. The sub-problem (6) can be solved using the normal equations:

$$x_{n+1} = (A^H A + \lambda I)^{-1} (A^H (b) + \lambda z_n) \quad (8)$$

Equation(5) is Recursive Network Module, its construction shows as Figure.6. Equation(6) is Data Consistency Module, which consists of  $A^H A + \lambda I$  and Conjugate Gradient.

Fig.6-8 illustrate the MoDL architecture, which is a deep learning approach for reconstructing images. Figure.6 depicts the CNN-based block used for noise reduction, termed  $D_w$ . Figure.7 details the iterative MoDL strategy that toggles between the denoising  $D_w$  as shown in equation (7) and a layer ensuring data consistency (DC), described in equation (8). Finally, Figure.8 reveals the expanded structure for a preset number of  $K$  cycles, within which the denoising blocks  $D_w$  use a shared set of weights throughout.

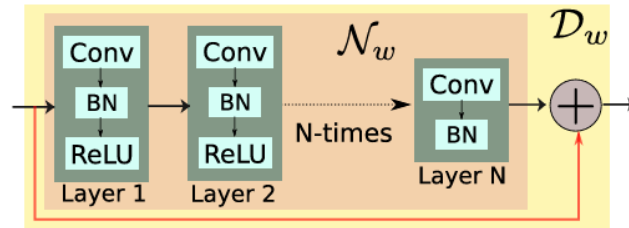


Figure 3: The residual learning based denoiser.

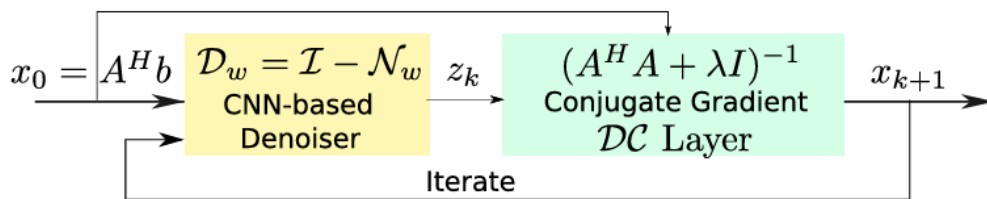


Figure 4: Proposed Model-based Deep Learning(MODL) architecture.

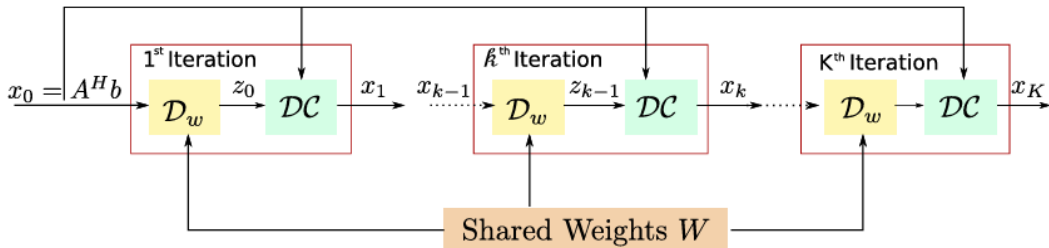


Figure 5: Unrolled architecture as described in equation(6).

### 4.3 SSDU

Because original SSDU code running on the tensorflow, we need to convert the code to run on the Py\_Torch that implement SSDU on the project "MoDL\_PyTorch"(PyTorch). The optimization problem in SSDU is:

$$\arg \min_x \|y_\Omega - E_\Omega x\|_2^2 + \mathcal{R}(x) \quad (9)$$

where  $E_\Omega$  is forward operator,  $y_\Omega$  is measured  $k$ -space data and  $\mathcal{R}(x)$  is a regularization term. The optimization problem in Equation (9) can be solved in variable splitting with quadratic penalty [5] for implementation. So the alternating optimization algorithms:

$$x_{\text{rec}} = \arg \min_{x,z} \|y_\Omega - E_\Omega x\|_2^2 + \mu \|x - z\|_2^2 + \mathcal{R}(z) \quad (10)$$

So the upgrade rules in SSDU:

$$z^{(i-1)} = \arg \min_z \mu \|x^{(i-1)} - z\|_2^2 + \mathcal{R}(z) \quad (11)$$

$$x^{(i)} = \arg \min_x \|y_\Omega - E_\Omega x\|_2^2 + \mu \|x - z^{(i-1)}\|_2^2 \quad (12)$$

where  $i$  is cascade index,  $z$  is the auxiliary variable that is initially constrained to be equal to  $x$ , and  $\mu$  is the parameter for the quadratic penalty for relaxing this intermediate constrained problem to an unconstrained one. A closed-form solution for The DC subproblem in Equation (12):

$$x^{(i)} = (E_\Omega^H E_\Omega + \mu I)^{-1} (E_\Omega^H y + \mu z^{(i-1)}) \quad (13)$$

Figure.7-8 showcases an iterative optimization strategy typically employed for solving inverse reconstruction problems with regularization. In Figure.7, This process oscillates between regularization (R) and ensuring data consistency (DC), executing a predetermined number of steps, and leading to a sequential architecture comprising both R and DC components. In Figure.8 The R component, in this case, is realized through a neural network architecture that includes 15 residual blocks. Each block is composed of a pair of convolutional layers—the first is succeeded by a rectified linear unit (ReLU) and the second by a layer performing scalar multiplication.

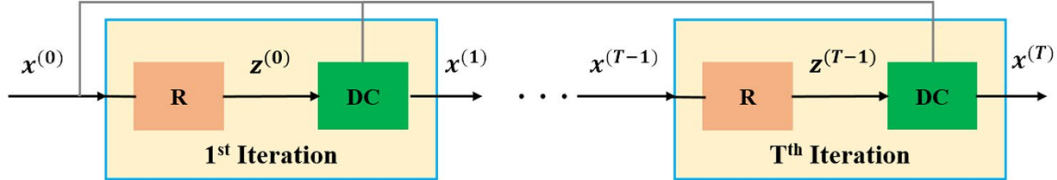


Figure 6: Unrolled neural network architecture as described in equation(12).

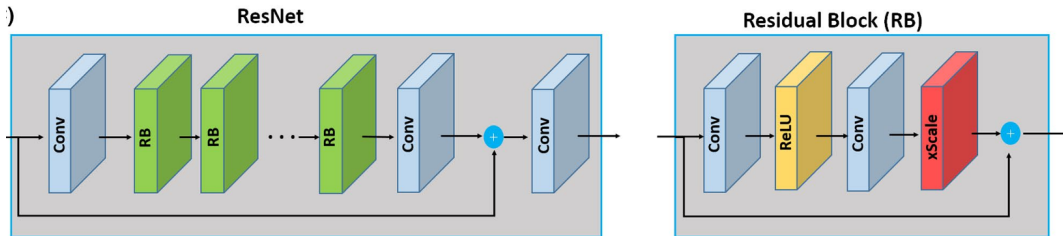


Figure 7: The Resnet architecture.

## 5 Results and Discussion

### 5.1 VARNET

In Figure.8, VARNET consists of 5 layers, 50 epochs MSE loss function and Adam optimization with 0.001 lr. Figure.8 demonstrates how image reconstruction quality can be significantly influenced by the  $k$ -iterations in MRI scans when using a deep learning model such as VARNET. With an acceleration factor of  $k=1$ , the reconstructed image retains most of the high-fidelity features from the ground truth (GT), evidenced by a PSNR of 33.3228 and an SSIM of 0.9050, which are indicative of minimal loss in detail and contrast. As the acceleration factor increases to  $k=5$ , there is a noticeable decline in the clarity and detail of the reconstructed image; the PSNR drops to 23.1528 and the SSIM to 0.6787, pointing to a compromise in reconstruction accuracy. At  $k=10$ , the trade-off becomes even more pronounced—the PSNR plummets to 18.9662 and the SSIM to 0.4320, showing significant artifacts and a loss of structural details. This diminishing quality is a consequence of the accelerated process that captures less  $k$ -space data, necessitating a more robust algorithm to maintain image integrity. The trade-off illustrated here emphasizes the need for optimizing the reconstruction process to achieve an acceptable balance between scan time reduction and image quality.

In Figure.9, VARNET consists of 5 layers, 1  $k$ -iteration MSE loss function and Adam optimization with 0.001 lr. Figure.9 demonstrates a clear trend of image improvement correlating with the number of epochs in the machine learning model training. Starting with the ground truth (GT) as the benchmark, the reconstruction at epoch 20 shows decent resemblance, but there's a visible difference in the crispness and fine details. At epoch 50, the PSNR and SSIM values have improved, indicating a reconstruction closer to GT, with better-defined edges and contrast. By epoch 80, the reconstruction is almost indistinguishable from GT, with PSNR and SSIM values surpassing those at epoch 50. This signifies that as the model goes through more training epochs, it becomes more adept at capturing the nuances and structures of the brain tissue, leading to a higher fidelity in the reconstructed image. It demonstrates the model's learning curve and the importance of sufficient training time for deep learning models tasked with complex image reconstructions like MRI brain scans. The continuous rise in both PSNR and SSIM suggests that the model, with more training, could potentially improve even further.

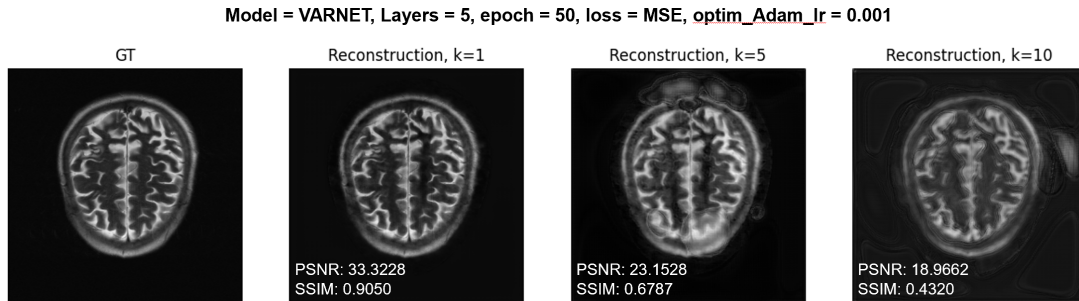


Figure 8: Reconstruction Image of VARNET with different  $k$ -iterations.

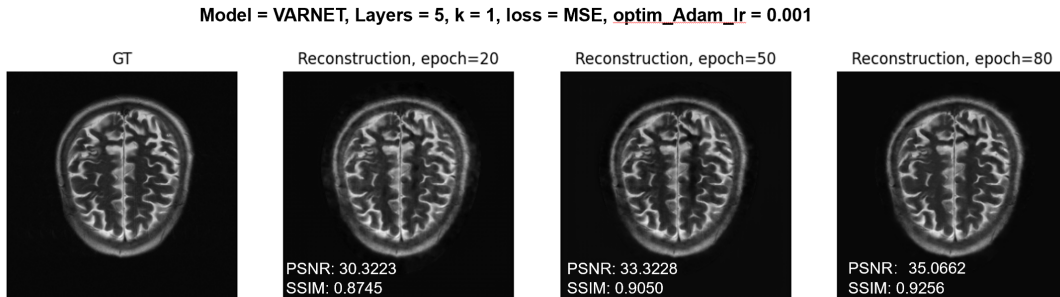


Figure 9: Reconstruction Image of VARNET with different epochs.

## 5.2 MODL

In Figure.10, VARNET consists of 5 layers, 50 epochs MSE loss function and Adam optimization with 0.001 lr. Figure.10 provides an interesting insight into the performance of the MODL model for MRI image reconstruction at different  $k$ -iterations. The GT presents a clear and detailed brain structure, which serves as a benchmark for the reconstructed images. At  $k=1$ , after 50 epochs of training, the reconstruction is very close to the GT with a high PSNR and SSIM, indicating excellent quality retention.

As we increase the  $k$ -iterations to  $k=5$ , the quality degrades significantly, illustrated by the SSIM dropping below 0.1. Such a low SSIM value generally points to a loss of structural integrity in the image, which is corroborated by the visual difference from the GT. However, the PSNR shows a highly unusual negative value, which is typically not possible and suggests a potential error in either the computation or the reporting of the metric.

At  $k=10$ , the reconstruction suffers further, with the PSNR and SSIM values indicating a severe loss of image quality. The reconstruction exhibits blurring and loss of definition, making it the least accurate representation of the original GT among the three. The progression from  $k=1$  to  $k=10$  starkly illustrates the trade-offs required when accelerating MRI scans — as the  $k$ -factor increases, the difficulty in accurately reconstructing the image also rises.

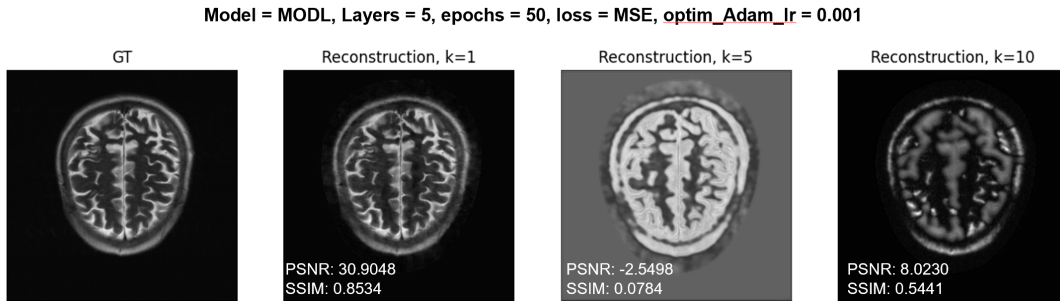


Figure 10: Reconstruction Image of MODL with different  $k$ -iterations.

In Figure.11, MODL consists of 50 epochs, 1  $k$ -iteration, MSE loss function and Adam optimization with 0.001 lr. we can delve deeper into the subtle intricacies of the reconstruction process using the MODL framework. The GT image provides a baseline for assessing the reconstructed images. At 5 layers and 50 epochs, the model performs well, with a PSNR close to 31, suggesting a good restoration of the image from the compressed or incomplete data. As we increase the layers to 10 and then to 20, we might expect a more nuanced capture of features due to the increased capacity for complexity; however, the PSNR and SSIM metrics indicate only a slight decrease in image quality. This could suggest that beyond a certain point, adding more layers does not yield significant improvements and might even introduce unnecessary complications or noise into the model, potentially due to overfitting or model complexity that exceeds the dataset's intrinsic information. The optimal model architecture for this task is likely to be one that strikes a balance between sufficient complexity to capture important features and simplicity to avoid overfitting, which underscores the critical importance of model tuning in the field of medical imaging.

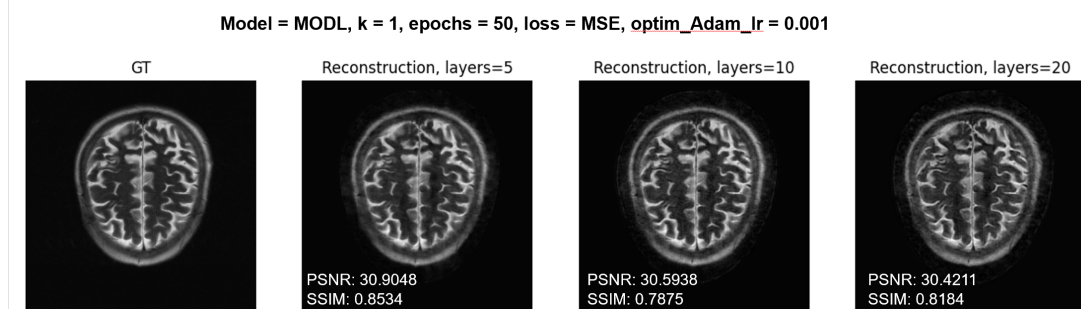


Figure 11: Reconstruction Image of MODL with different layers.



### 5.3 SSDU

In Figure.12, SSDU consists of 15 layers, 50 epochs, 1 k-iteration and L1L2 loss function. Figure.12 illustrates varying levels of clarity and detail captured by the MODL deep learning model at different learning rates, after training for 50 epochs. The ground truth (GT) image sets a high standard of detail and contrast for comparison.

The first reconstruction at  $\text{optimi\_lr}=0.0001$  shows a moderate fidelity to the GT with PSNR and SSIM scores that are fairly decent, indicating a good level of detail preservation. However, as the learning rate increases to 0.001, the PSNR decreases slightly, suggesting some loss of image quality, while the SSIM increases, which could imply a slight improvement in the structural integrity of the reconstructed image.

Strikingly, at  $\text{optimi\_lr}=0.005$ , the PSNR is deeply negative. Normally, the PSNR should be a positive value; its negative value here suggests a significant discrepancy from the GT and possibly points towards a calculation error or an issue with the image reconstruction at this learning rate.

This spread of reconstructions highlights the sensitivity of the learning rate in deep learning applications for medical imaging. It's a critical parameter that can significantly affect the model's ability to learn and replicate the intricate details necessary for accurate diagnosis. It underscores the fine balance required in tuning deep learning models for such precision tasks, where both over- and under-estimation of parameter values can lead to suboptimal results.

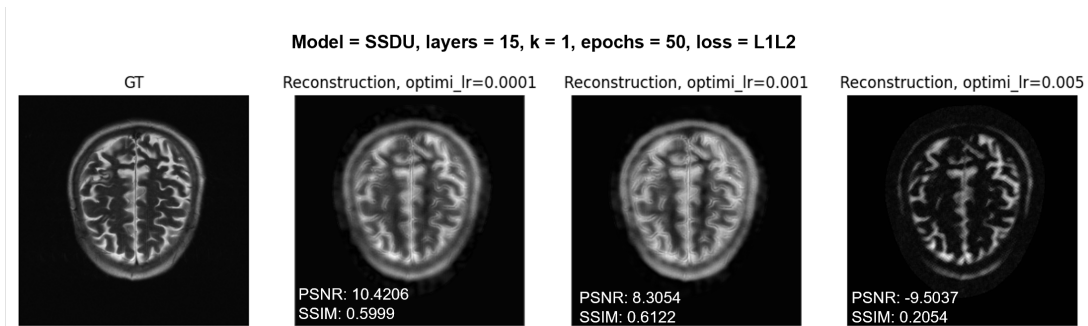


Figure 12: Reconstruction Image of SSDU with different  $\text{optimi\_lr}$  when  $k=1$ .

In Figure.13, SSDU consists of 15 layers, 50 epochs, 10  $k$ -iteration and L1L2 loss function. Figure.13 illustrates the performance of the MODL deep learning model on MRI brain scan reconstructions at various learning rates after 50 epochs. The ground truth (GT) scan provides a reference standard showcasing a clear and detailed cerebral anatomy.

In the first reconstruction at an  $\text{optimi\_lr}$  of 0.0001, the resulting image has a relatively low PSNR of 11.5523, suggesting considerable deviation from the GT. The SSIM, while moderate, indicates a loss in image structure and detail.

At an  $\text{optimi\_lr}$  of 0.0005, the image quality substantially improves, reflected by a higher PSNR of 27.2587, which is more indicative of a faithful reconstruction. The SSIM also sees a significant increase, implying better structural integrity that aligns more closely with the GT.

When the learning rate is increased to 0.001, there is a decline in PSNR, indicating that the image quality has worsened relative to the previous learning rate. However, the SSIM remains relatively high, suggesting that some structural elements are still well-preserved.

This demonstrates the sensitivity of learning rates in image reconstruction tasks. The right learning rate can improve the model's ability to learn detailed features without introducing noise, whereas an inappropriate rate can lead to suboptimal results, capturing less detail and causing a degradation in image quality. The nuanced balance in selecting a learning rate is key to maximizing a model's performance in reconstructing medical images.

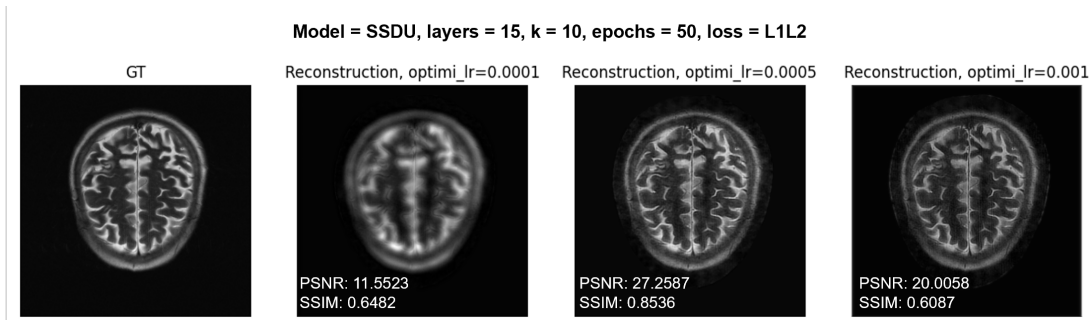


Figure 13: Reconstruction Image of SSDU with different optimi\_lr when  $k=10$ .

In Figure.14, SSDU consists of 15 layers, 50 epochs, L1L2 loss function and dam optimization with 0.001 lr. Figure.14 offers a comparative view of MRI brain scans reconstructed with the SSDU model at different  $k$ -iterations ( $k=1$ ,  $k=5$ ,  $k=10$ ), reflecting varying levels of image clarity and detail.

Starting with the GT, the reconstruction at  $k=1$  has a significantly lower PSNR, suggesting a substantial loss of detail. Yet, its SSIM indicates a moderate preservation of structural integrity, hinting that while the overall luminance and contrast are affected, the image maintains a semblance of the original structure.

As the  $k$ -iterations increases to  $k=5$ , there’s a notable improvement in PSNR, suggesting that despite faster acquisition, the model is capturing more details accurately. Interestingly, the SSIM sees an improvement, which is counterintuitive as higher acceleration usually leads to more loss of structural fidelity.

At  $k=10$ , the PSNR drops, signifying that as the acquisition speed increases, the image quality decreases. However, the SSIM is slightly better than at  $k=1$ , indicating that the model still retains some structural elements of the brain despite the accelerated scanning process.

Overall, these reconstructions demonstrate the challenge in balancing scan speed with image quality and the potential of advanced reconstruction algorithms to mitigate the trade-offs involved in accelerated MRI techniques. The SSDU model seems to handle the acceleration well up to a certain point, beyond which the image quality diminishes rapidly, underscoring the need for careful optimization of the acceleration factor in clinical settings.

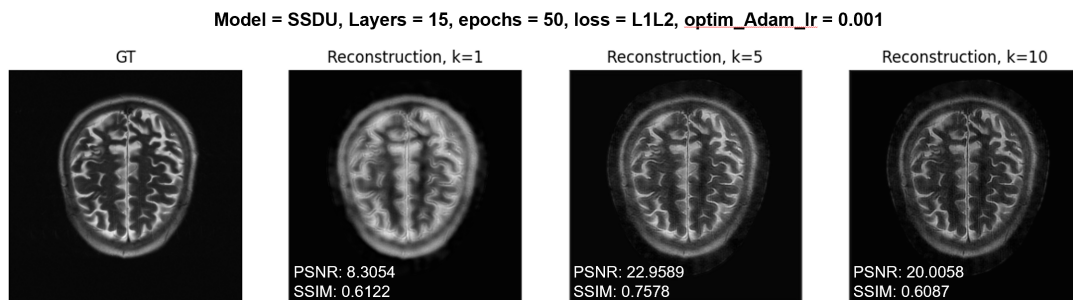


Figure 14: Reconstruction Image of SSDU with different  $k$ .

## 5.4 Compare VARNET, MODL, SSDU

In Figure.15, three different models—VARNET, MODL, and SSDU—are used for image reconstruction, and their outcomes are compared against the ground truth (GT). The VARNET reconstruction aligns closely with the GT, with a high PSNR and SSIM, indicating minimal loss of image quality and structural integrity. The MODL model also performs well, with a slight drop in PSNR and SSIM, but still maintains a strong resemblance to the GT. In contrast, the SSDU model’s reconstruction has a significantly lower PSNR, which suggests a greater loss of image detail and accuracy. The SSIM is higher than the PSNR might suggest, which means some structural aspects of the image are preserved, but the overall quality is much lower compared to the other models. This comparative analysis underscores the strengths and weaknesses of different reconstruction approaches and highlights the importance of selecting an appropriate model for the desired level of image quality in medical imaging tasks.

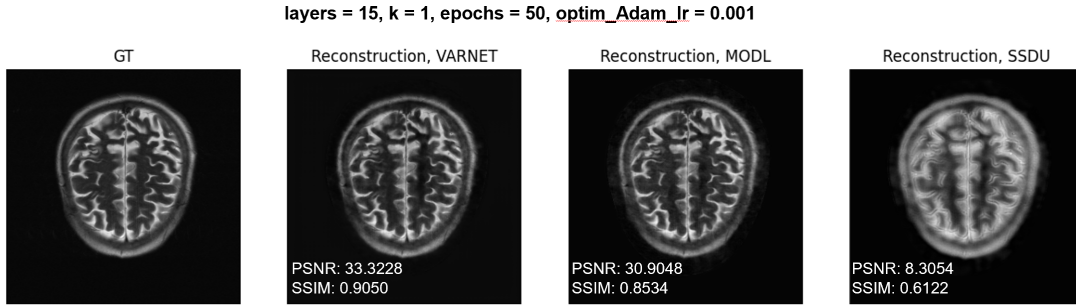


Figure 15: Comparison of different models with  $k=1$ .

Figure.16 showcases the outcomes of different deep learning reconstruction methods at  $k$ =iterations ( $k$ ) of 10, which is quite high, indicating a faster but potentially less detailed scan. The ground truth (GT) offers a sharp and detailed reference for comparison.

The VARNET model’s reconstruction presents a significant drop in detail and clarity from the GT, reflected in both the PSNR and SSIM scores. MODL’s approach, while marginally better in terms of PSNR, still portrays a significant deviation from the GT, with considerable image artifacts and a lower SSIM. The SSDU reconstruction, however, even though it has a higher PSNR than MODL, depicts the lowest SSIM, implying a greater loss in the structural integrity and texture details of the image.

This analysis indicates that higher acceleration factors greatly challenge the reconstruction models, as they must work with substantially less data to recreate the image. The discrepancies in image quality between the methods suggest varying efficacies in handling such sparse data. Moreover, the loss of fine details critical for diagnostic accuracy in clinical settings is a crucial factor when considering the practical application of these accelerated MRI techniques. Each method’s ability to preserve critical diagnostic information must be weighed against the speed of image acquisition.

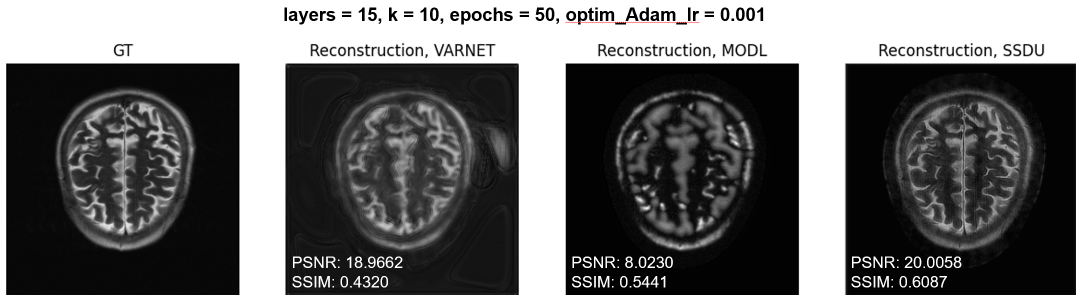


Figure 16: Comparison of different models with  $k=10$ .

## 6 Conclusion

In conclusion, the research undertaken in this computational imaging project elucidates the significant advancements and challenges in the field of MRI reconstruction. By comparing and contrasting three sophisticated approaches—VARNET, MODL, and SSDU—the study delves deep into the mechanics and outcomes of these models, showcasing their unique strengths and potential limitations in the context of accelerated MRI data reconstruction.

VARNET, with its variational network approach, demonstrates exceptional capability in maintaining image quality at lower  $k$ -iterations, a testament to its effective integration of deep learning with variational models. MODL, leveraging model-based deep learning, illustrates its strength in reconstructing high-quality images from sparse datasets, pointing to its potential in reducing MRI scan times and improving patient experience. SSDU, through its self-supervised learning strategy, presents a novel methodology that challenges traditional supervised learning paradigms and offers a pathway to reconstruct images where fully sampled datasets are not available.

This comparison not only highlights the technological strides made in computational imaging but also underscores the importance of selecting appropriate reconstruction algorithms tailored to specific clinical needs. The balance between  $k$ -iteration and image fidelity remains a pivotal challenge; however, the innovative approaches explored in this project offer promising solutions that could revolutionize MRI reconstruction techniques, thereby enhancing diagnostic accuracy and patient care.

The evolution of MRI reconstruction, as showcased in this project, is a vibrant area of research that continues to push the boundaries of medical imaging technology. As these computational imaging models evolve, further studies will be essential to refine their capabilities, improve their integration into clinical workflows, and ultimately, harness the full potential of MRI technology to better serve patients and medical professionals alike.

## References

- [1] K. Hammernik, T. Klatzer, E. Kobler, M. P. Recht, D. K. Sodickson, T. Pock, and F. Knoll, “Learning a variational network for reconstruction of accelerated mri data,” *Magnetic resonance in medicine*, vol. 79, no. 6, pp. 3055–3071, 2018.
- [2] H. K. Aggarwal, M. P. Mani, and M. Jacob, “Modl: Model-based deep learning architecture for inverse problems,” *IEEE transactions on medical imaging*, vol. 38, no. 2, pp. 394–405, 2018.
- [3] B. Yaman, S. A. H. Hosseini, S. Moeller, J. Ellermann, K. Uğurbil, and M. Akçakaya, “Self-supervised learning of physics-guided reconstruction neural networks without fully sampled reference data,” *Magnetic resonance in medicine*, vol. 84, no. 6, pp. 3172–3191, 2020.
- [4] M. Uecker, P. Lai, M. J. Murphy, P. Virtue, M. Elad, J. M. Pauly, S. S. Vasanawala, and M. Lustig, “Espirit—an eigenvalue approach to autocalibrating parallel mri: where sense meets grappa,” *Magnetic resonance in medicine*, vol. 71, no. 3, pp. 990–1001, 2014.
- [5] M. V. Afonso, J. M. Bioucas-Dias, and M. A. Figueiredo, “Fast image recovery using variable splitting and constrained optimization,” *IEEE transactions on image processing*, vol. 19, no. 9, pp. 2345–2356, 2010.